Primary Breakup of Turbulent Round Liquid Jets in Uniform Crossflows

K. Lee[*] and C. Aalburg[†]
*University of Michigan, Ann Arbor,
Michigan 48109-2140*
F. J. Diez[‡]
*Rutgers, the State University of New Jersey,
Piscataway, New Jersey 08854*
G. M. Faeth[§]
University of Michigan, Ann Arbor, Michigan 48109-2140
and
K. A. Sallam[¶]
Oklahoma State University, Stillwater, Oklahoma 74078

An experimental investigation of the deformation and breakup properties of turbulent round liquid jets in uniform gaseous crossflows is described. Pulsed shadowgraph and holograph observations were obtained for turbulent round liquid jets injected normal to air crossflow in a shock tube. Crossflow velocities of the air behind the shock wave relative to the liquid jet were subsonic (36–90 m/s) and the air in this region was at normal temperature and pressure. Liquid injection was done by a pressure feed system through round tubes having inside diameters of 1 and 2 mm and length-to-diameter ratios greater than 100 to provide fully developed turbulent pipe flow at the jet exit. Test conditions were as follows: water and ethyl alcohol as test liquids, crossflow Weber numbers based on gas properties of 0–282, streamwise Weber numbers based on liquid properties of 1400–32,200, liquid/gas density ratios of 683 and 845, and jet exit Reynolds numbers based on liquid properties of 7100–48,200, all at conditions in which direct effects of liquid viscosity were small (Ohnesorge numbers were less than 0.12). Measurements were carried out to determine conditions required for the onset of breakup, ligament and drop sizes along the liquid surface, drop velocities after breakup, liquid column breakup as whole, rates of turbulent primary breakup, and liquid column trajectories. Phenomenological theories proved to be quite successful in interpreting and correlating the measurements.

Nomenclature

C_D	=	drag coefficient
C_i, C_i'	=	coefficient for property i of the turbulent primary breakup
d	=	round jet exit diameter
d_{lig}	=	ligament diameter
d_p	=	drop diameter
L	=	length of the constant-diameter portion of the injector passage
L_c	=	mean liquid jet breakup length
$\dot{m}_L''$	=	liquid breakup mass flux
n	=	power in the breakup property expressions
Oh	=	Ohnesorge number, $\mu_L/(\rho_L d\sigma)^{1/2}$
q	=	liquid/gas momentum ratio, $\rho_L v_j^2/(\rho_G u_\infty^2)$
Re	=	liquid jet Reynolds number, $\rho_L v_j d/\mu_L$
SMD	=	Sauter mean diameter of drops
t_b	=	time required for the liquid column breakup as a whole
t_r	=	Rayleigh breakup time
t^*	=	characteristic aerodynamic time, $(\rho_L/\rho_G)^{1/2}d_j/u_\infty$
u	=	cross-stream velocity
v	=	streamwise velocity
We_G	=	crossflow Weber number, $\rho_G d u_\infty^2/\sigma$
We_L	=	streamwise Weber number, $\rho_L d v_j^2/\sigma$
$We_{L\Lambda}$	=	Weber number based on the jet exit radial (cross-stream) integral length scale, $\rho_L \Lambda v_j^2/\sigma$
x	=	cross-stream distance
y	=	streamwise distance
ε	=	surface efficiency factor
Λ	=	radial (cross-stream) integral length scale
μ	=	molecular viscosity
ρ	=	density
σ	=	surface tension

Subscripts

b	=	location of the liquid column breakup as a whole
G	=	gas property
i	=	location of the onset of the breakup
j	=	jet exit property
L	=	liquid property
lig	=	ligament property
p	=	property of the drops formed by the primary breakup
surf	=	liquid surface property
∞	=	ambient gas property

*Research Fellow, Department of Aerospace Engineering. Member AIAA (Corresponding Author).
†Currently GE Global Research, Munich, Germany.
‡Assistant Professor, Department of Mechanical and Aerospace Engineering. Senior Member AIAA.
§A. B. Modine Distinguished University Professor (Deceased), Department of Aerospace Engineering. Fellow AIAA.
¶Assistant Professor, School of Mechanical and Aerospace Engineering. Member AIAA.

I. Introduction

THIS research was motivated by applications to the primary breakup of liquid jets in crossflow encountered in airbreathing propulsion systems, liquid rocket engines, diesel engines, spark ignition engines, and agricultural sprays, among others. Recent experimental and computational studies of Mazallon et al. [1], Sallam et al. [2], and Aalburg et al. [3] considered the deformation and breakup properties of nonturbulent round liquid jets in uniform gaseous crossflows, and Fuller et al. [4] studied the effect of injection angle on turbulent liquid jets in uniform air crossflow. The objective of the present investigation was to extend these results to consider the primary breakup of turbulent liquid jets in uniform gaseous crossflows, because most practical sprays involve some level of turbulent disturbance in the liquid jet leaving the injector exit. To control the scope of the present study, jet exit turbulence was at the well-defined limit of fully developed turbulent pipe flow, which is representative of high Reynolds number injector flows for large length/diameter ratio injectors.

Early studies of the primary breakup of nonturbulent round liquid jets in uniform gaseous crossflows have been recently reviewed by Aalburg et al. [3] and references cited therein; therefore, the present review of this literature will be limited to recent studies. Mazallon et al. [1], and Sallam et al. [2] considered the primary breakup of nonturbulent liquid jets with large liquid/gas density ratios based on experiments using pulsed shadowgraph and pulsed holograph observations of primary breakup regimes (conditions required for the onset of ligament and drop formation, ligament and drop sizes along the liquid surface, drop velocities after breakup, rates of liquid breakup between the onset of drop formation and the breakup of the liquid column as a whole, the breakup of the liquid column as a whole, and liquid column trajectories), all for subsonic air crossflows at normal temperature and pressure (NTP). The results suggested qualitative similarities between the primary breakup of nonturbulent round liquid jets in gaseous crossflow and the secondary breakup of drops subjected to shock wave disturbances. It was also found that phenomenological analyses were effective to help interpret and correlate the measurements. This research was extended by the computational and experimental study of the deformation and breakup properties of nonturbulent round liquid jets in uniform gaseous crossflows by Aalburg et al. [3] that addressed the breakup properties at a higher density ratio and sought to use computations to study aspects of breakup that are difficult to address by experiments. Aalburg et al. concluded that liquid/gas density ratios had little effect on the deformation and breakup regime boundaries of nonturbulent round liquid jets in crossflows and that there was a significant increase of the resistance of liquid jets to deformation when the crossflow Reynolds number approached small values typical of the Stokes flow regime. At large Ohnesorge numbers, breakup regime boundaries were found to scale according to a new nondimensional number that relates liquid viscous forces to surface tension forces as opposed to the Weber number, which relates drag forces to surface tension forces and which is the classical scaling approach for small Ohnesorge number conditions. Fuller et al. [4] experimentally studied effects of injection angle on column breakup and trajectories of turbulent round liquid jets in crossflows and divided column breakup behavior into aerodynamic and nonaerodynamic regimes. However, effects of liquid turbulence on the deformation and breakup properties of round liquid jets in crossflow were not investigated in these studies; this is unfortunate, because most practical liquid injectors introduce some degree of turbulence in the liquid jet leaving the injector passage.

Drop formation along the surface of turbulent liquids, called turbulent primary breakup, is a common mechanism of spray formation in industrial and natural processes (e.g., spray atomization, bow waves of ships, whitecaps, etc.). The turbulent primary breakup

mechanism was first identified by De Juhasz et al. [5] and Lee and Spenser [6,7]. Subsequent studies by Schweitzer [8], Chen and Davis [9], Grant and Middleman [10], Phinney [11], McCarthy and Malloy [12], and Hoyt and Taylor [13,14] confirmed that liquid turbulence affects spray properties and that turbulent primary breakup dominates the formation of ligaments and drops near the surface of turbulent liquids in still or slowly moving gases at NTP.

Subsequent studies by Wu et al. [15–18], Dai et al. [19], Sallam et al. [20,21], and Sallam and Faeth [22] used pulsed shadowgraphy and pulsed holography to study the properties of turbulent primary breakup for fully developed turbulent liquid jets injected in still gases for a variety of liquid jet geometries. The main findings were as follows: aerodynamic effects were small for liquid/gas density ratios greater than 500; drop size distributions after turbulent primary breakup satisfied the universal root normal distribution of Simmons [23] and were completely defined by the Sauter mean diameter (SMD) of the sprays; drop velocities after breakup were independent of drop size and were related to the mean turbulent liquid jet exit velocities; and the drop and ligament sizes along the liquid surface and the rate of liquid breakup along the liquid surface could be interpreted and correlated based on simplified phenomenological analyses. None of these studies included consideration of gas flows across the turbulent liquid surface sufficient to introduce significant aerodynamic effects.

The objective of the present investigation was to extend the studies of liquid breakup for nonturbulent round liquid jets in crossflow [1–3] and turbulent primary breakup of liquids in the presence of negligible aerodynamic effects [15–22], to consider the breakup properties of turbulent round liquid jets in uniform crossflows, using experimental methods similar to those of the past work. To control the scope of the study, breakup was considered in uniform air crossflows at NTP, with liquid turbulence limited to fully developed turbulent pipe flow at the injector exit. Finally, phenomenological analyses were used to help interpret and correlate the measurements.

The following description of the investigation begins with consideration of experimental methods. Results are then discussed considering breakup regimes, liquid surface velocities, conditions required for the onset of liquid breakup along the liquid jet surface, the variation of ligament and drop sizes along the liquid surface, the variation of drop velocities along the liquid surface, liquid column breakup as whole, the variation of the rates of liquid breakup along the liquid surface, and liquid column trajectories.

II. Experimental Methods

A. Test Apparatus

Observations of liquid breakup along the surface of a round liquid jet were carried out using a shock tube apparatus, as sketched in Fig. 1. The shock tube had a rectangular cross section with a width of 38 mm and a height of 64 mm. The driven section of the shock tube was open to the atmosphere and had windowed side walls to provide optical access. The shock tube was sized to provide test times of 17–20 ms in the uniform subsonic flow region behind the shock wave. Crossflow velocities of 36–90 m/s in air at NTP were considered.

Pressure injection was used to feed the test liquids from a cylindrical storage chamber into round nozzles directed vertically downward across the midplane of the shock tube. The injector system for fully developed turbulent round liquid jets in uniform gaseous crossflows is sketched in Fig. 1. The storage chamber had an inside diameter and height of 50 and 100 mm, respectively. The nozzles had smooth rounded entrances with length-to-diameter ratios greater than 100 to insure fully developed turbulent pipe flow at the jet exit for sufficiently large liquid jet Reynolds numbers, as discussed by Wu and Faeth [16] and references cited therein.

The test liquid was placed in the storage chamber through a port with premature outflow prevented by surface tension forces at the injector exit. The liquid was forced through the nozzle by admitting high-pressure air to the top of the chamber through a solenoid valve. The high-pressure air was stored in an accumulator having a volume
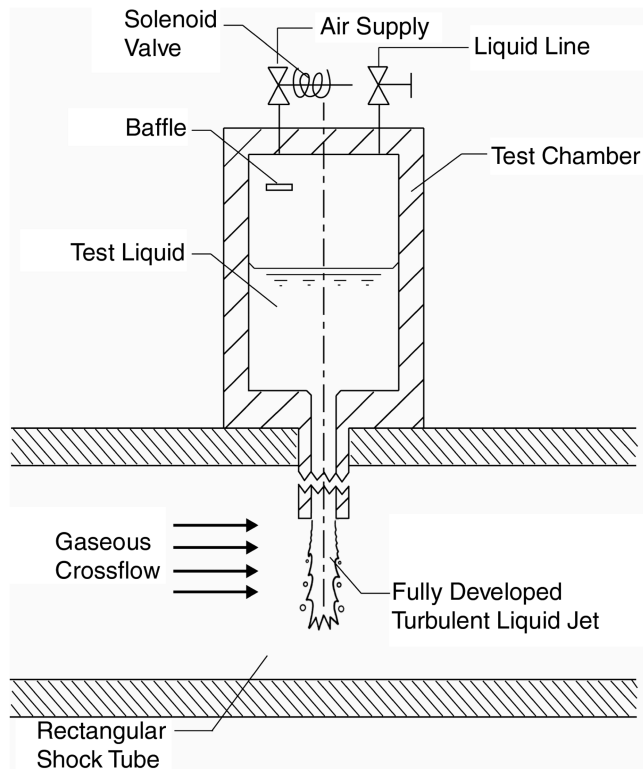
Fig. 1 Sketch of the injector system for fully developed turbulent round liquid jets in uniform gaseous crossflows.

of 1.3 m³ on the upstream side of the solenoid valve, with provision for accumulator air pressures up to 1.5 MPa (with air dew points smaller than 240 K). Significant aeration of the test liquid was prevented in several ways: a baffle was placed across the air inlet of the liquid supply chamber, the cross-sectioned area of the supply chamber was large compared with the injector tube cross-sectional area (streamwise liquid velocities in the chamber were less than 7 mm/s), and liquid during the present observations was drawn from the bottom of the liquid supply chamber, well away from the liquid surface. Notably, these steps were sufficient to prevent observation of bubbles in the liquid for the observations of nonturbulent liquid jets of Sallam et al. [2]. Once all the liquid was forced out of the liquid supply chamber, the solenoid valve was closed and the liquid supply chamber was refilled for the next test.

Test times were short for the shock tube arrangement, less than 20 ms. However, this was not a problem because flow development times (the time required for a given liquid sample to cross the flow cross section) were smaller than one-third of available test times. In addition, data acquisition times, using pulsed shadowgraphy and holography, were even shorter, less than 10 ns, and did not impose any significant test time requirements.

The uniformity of the crossflow acting on the round liquid jets is an important issue discussed by Mazallon et al. [1]. For the present results, measurements were obtained at short times (less than 20 ms) after passage of the shock wave past the liquid jet locator. As a result, the thickness of the nonuniform velocity field in the boundary layer along the shock tube walls was generally less than 0.5 mm, based on the transient analysis presented by Schlichting [24]. In addition, the injector tube was shifted normal to the wall to observe the flow at various positions along the liquid jet; as a result, the disturbed region along the wall was smaller than 10% of the distance along the liquid jet for all observations made during the present investigation.

B. Instrumentation

Pulsed shadowgraphy and pulsed holography were used for all observations of the liquid surface and its breakup properties during the present investigation. The light sources for shadowgraphy and holography were two frequency-doubled YAG lasers with 7-ns pulse

duration and 300-mJ optical energy per pulse. Pulse separations could be as small as 100 ns. Ligament and drop sizes were measured using single-pulsed shadowgraphy, whereas surface and drop velocities were obtained from double-pulse shadowgraphy images by measuring the displacement of surfaces or the motion of the centroid of the drops. The shadowgraphs were recorded using Polaroid types 55 and 57 black-and-white film, and data were obtained by mounting the images on a x–y traversing system and observing the images with a charge-coupled device (CCD) camera. To avoid problems of depth-of-field corrections, single-pulse off-axis holography was used to find the liquid breakup rates. The holograms were recorded on AGFA 8E75HD-NAD holographic glass plates and reconstructed using a 35-mW HeNe laser. The x–y traversing of the hologram was supplemented by z traversing of the video camera. Further details of the instruments and data processing methods have been fully described by Sallam et al. [2,20,21].

Ligament properties were found to be similar to those of Sallam et al. [21], and drop properties after primary breakup were found to be similar to those of Sallam et al. [2,20] Ligaments were approximately cylindrical and could be represented by their average diameters and lengths. Drops generally were spherical and could be completely described by the SMD under the approximations of the universal root normal drop size distribution function of Simmons [23]. Experimental uncertainties (95% confidence) were found using standard methods similar to past work [2,20,21]. These uncertainties were less than 10% for ligament and drop diameters larger than 10 μm, increasing inversely proportional to the diameter for smaller-sized objects. Drop velocities were found from simple arithmetic averages (because drop-velocity distributions as a function of size were nearly uniform), with experimental uncertainties (95% confidence) less than 10%. In all cases, the numbers of drops or ligaments measured at a point were chosen to comply with the experimental uncertainties (95% confidence) less than 10%. The same procedure was applied with all measured quantities including the breakup lengths and surface velocities, which were also measured with experimental uncertainties (95% confidence) less than 10%.

C. Test Conditions

Test conditions are summarized in Table 1. Liquid properties appearing in Table 1 were measured as follows: liquid densities using a set of precision hygrometers (Fisher Model 11–582, 0.1% accuracy), liquid viscosities using a Cannon–Fenske viscometer (Fisher Model 13–617, 3% accuracy), and surface tensions using a ring tensiometer (Fisher Model 20, 0.25% accuracy). The present results agreed with values appearing in Lange [25], within the accuracy of the instruments.

Test conditions were varied by considering two different liquids (water and ethyl alcohol), injector passage diameters of 1.0 and 2.0 mm, liquid jet velocities of 10–21 m/s, and air crossflow velocities of 36–90 m/s at NTP. This yielded the following ranges of

Table 1   Summary of test conditions[a]

Liquid	Water	Ethyl alcohol
Density, kg/m³	995	806
Liquid jet velocity, m/s	9.9–19.8	10.8–21.1
Liquid/gas density ratio, ρ_L/ρ_G	845	683
Liquid viscosity, kg/m · s × 10⁴	8.94	12.3
Liquid/gas viscosity ratio, μ_L/μ_G	48	66
Surface tension, N/m × 10³	70.8	24.0
Injector exit passage diameter, mm[b]	1.0, 2.0	1.0, 2.0
Liquid jet Reynolds number Re	12,100–48,200	7100–27,600
Crossflow Weber number We_G	0–159	0–282
Streamwise Weber number We_L	1400–11,000	4200–32,200
Liquid/gas momentum ratio q	3–200	20–100
Liquid jet Ohnesorge number, Oh × 10³	3–4	80–120

[a]Air crossflow at 98.8 kPa and 298 K; properties of air at normal temperature and pressure ($\rho_G = 1.18$ kg/m³ and $\mu_G = 18.5 \times 10^{-6}$ kg/m · s) and crossflow velocities of 36–90 m/s.
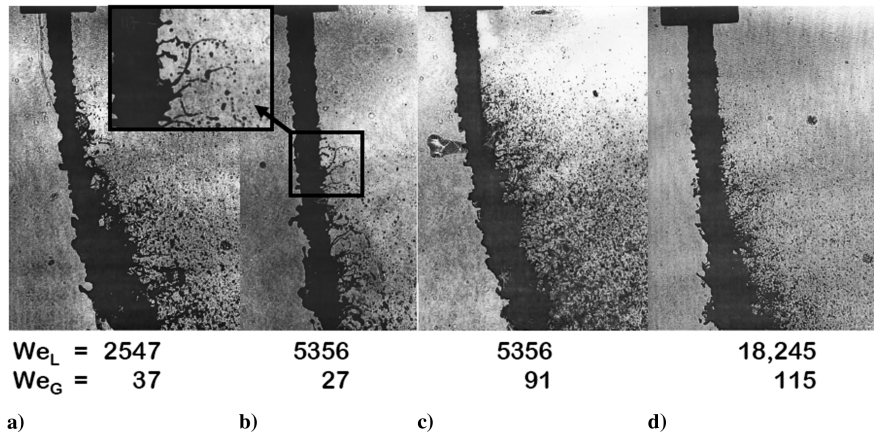[b]Injector passage length/diameter ratios greater than 100.

Fig. 2 Pulsed shadowgraphs of a–c) round water and d) alcohol jets in crossflowing air at three liquid turbulence levels (initial jet diameter $c_j = 1.1$ mm); the zoomed section illustrates the formation of ligaments with subsequent drop formation due to Rayleigh breakup.

test variables: liquid/gas density ratios of 683 and 845, liquid/gas momentum ratios q of 3–200, liquid jet Reynolds numbers Re of 7100–48,200; crossflow Weber numbers We_G of 0–282, streamwise Weber numbers We_L of 1400–32,200, and liquid jet Ohnesorge numbers Oh of 0.003–0.120. Crossflow Mach numbers were smaller than 0.3; therefore, compressibility effects were negligible.

III. Results and Discussion

A. Flow Visualization

Injector passage design, including the inlet contraction, the presence of trips and other turbulence-promoting devices, and the roughness and length of the constant-diameter portion of the injector passage, can modify conditions required for turbulent flow (and its degree of development) at the jet exit [16,24]. Naturally, these variables also control the nature of the turbulence at the injector exit. Thus, to control the number of test variables, the present experiments were limited to relatively long injector passages, $L/d > 100$, to achieve fully developed turbulent pipe flow for sufficiently large jet exit Reynolds numbers, as discussed by Wu et al. [17].

Visualization of the flow at the injector exit is provided by the pulsed shadowgraphs of round water and alcohol jets (Fig. 2). The initial jet diameters are $d_j = 1.1$ mm. Four exit conditions are shown. The liquid turbulence, represented by the liquid Weber number We_L, increases from left to right and is constant between Figs. 2b and 2c. The Weber number of the crossflow, We_G, is relatively constant between the first and the second picture and then increases from left to right. Under nonturbulent liquid jet conditions, the crossflow Weber numbers of Figs. 2a and 2b generally correspond to the bag or multimode breakup regime (see Sallam et al. [2]). The turbulent jets illustrated in Fig. 2, however, do not exhibit this behavior. Instead, the sole presence of ligaments without any bags is normally observed in the shear breakup regime of nonturbulent liquid jets in crossflows, which starts at Weber numbers $We_G \cong 110$. The visualizations thus illustrate the strong effect of the liquid turbulence on the breakup behavior of liquid jets in crossflow under the present test conditions. The increase in liquid turbulence from Fig. 2a to Fig. 2b enhances the formation of ligaments and subsequently drops. This effect, however, cannot be easily deduced from the pictures, because the liquid jet velocity has increased from left to right and so a direct correlation of jet conditions at similar distances from the nozzle is not possible.

The shadowgraph visualizations in Figs. 2b and 2c illustrate the effect of increasing crossflow velocities on a turbulent jet at constant liquid turbulence and liquid jet velocity levels. We_G increases from left to right, whereas We_L remains constant. Thus, a direct comparison between the two pictures is possible. The enhancing effect of the crossflow on the formation of ligaments and drops is evident. The pictures further show that drops are formed out of ligaments based on Rayleigh breakup and not as a result of Rayleigh–

Taylor or Kelvin–Helmholtz types of instabilities (see the zoomed section of Fig. 2b).

Figure 2d corresponds to conditions at large liquid turbulence and large crossflow Weber numbers. At these crossflow conditions, corresponding nonturbulent liquid jets are in the shear breakup regime and exhibit qualitatively similar behavior to the present illustration of a turbulent jet. Given the large liquid velocities, ligament and drop formations appear very rapidly.

B. Mean Liquid Column Breakup Lengths in Still Gases

Combined measurements of surface breakup regime boundaries for turbulent liquid jets in still air at NTP by Wu and Faeth [18] and the present investigation are illustrated in Fig. 3. Results shown on the plot pertain to three turbulent primary breakup conditions along the liquid surface, as follows: the breakup of the entire liquid column due to the turbulent primary breakup mechanism, L_c/d; the onset of turbulent primary breakup along the liquid surface, y_i/d; and the end of turbulent primary breakup along the liquid surface, y_e/d. The criterion for the liquid column length for turbulent primary breakup is given by Wu and Faeth as follows:

$$L_c/d = 8.51 We_L^{0.32} \qquad (1)$$

The correlations for y_i/d and y_e/d are similar to Eq. (1); see Wu and Faeth [18] for the correlations for each criterion. The present measurements were limited to the onset of turbulent primary breakup along the liquid surface and are seen to be in excellent agreement
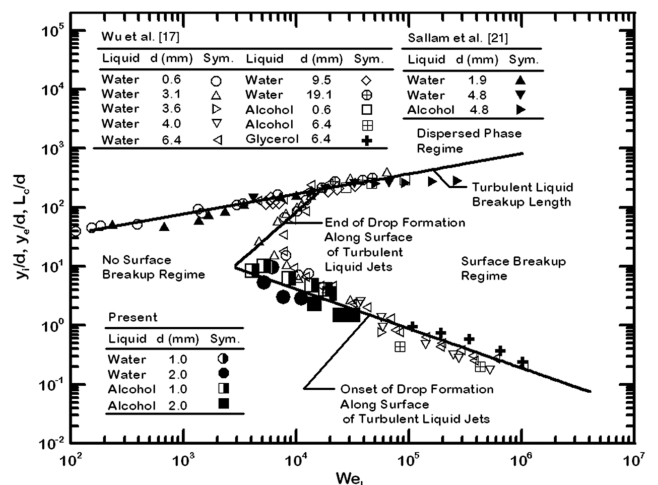

Fig. 3 Mean liquid column breakup lengths of turbulent round liquid jets in still air, plotted according to the turbulent liquid column breakup analysis of Sallam et al. [20] and the onset and end of liquid surface breakup analyses of Wu and Faeth [15].
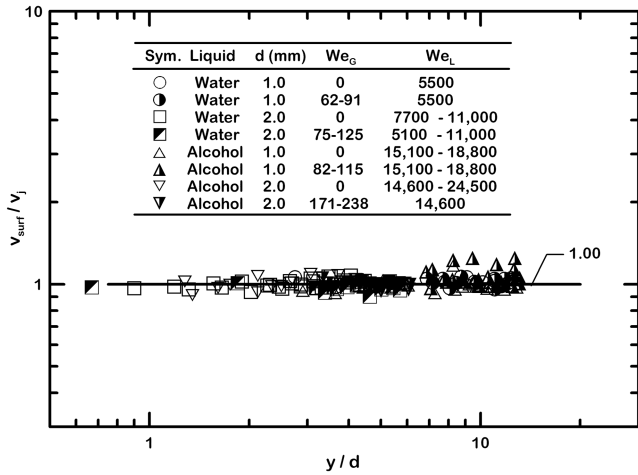
Sym.	Liquid	d (mm)	We$_G$	We$_L$
○	Water	1.0	0	5500
◐	Water	1.0	62-91	5500
□	Water	2.0	0	7700 - 11,000
◪	Water	2.0	75-125	5100 - 11,000
△	Alcohol	1.0	0	15,100 - 18,800
▲	Alcohol	1.0	82-115	15,100 - 18,800
▽	Alcohol	2.0	0	14,600 - 24,500
▼	Alcohol	2.0	171-238	14,600

Fig. 4 Mean liquid surface velocities as a function of the distance from the jet exit.

with the earlier measurements of Wu and Faeth for this condition. Finally, there are two other regimes for the length of the liquid column: Rayleigh-type breakup and bag/shear breakup of the liquid column. The present shock tube apparatus, however, was too confined to allow observation of liquid column breakup lengths in the absence of crossflow; see Sallam et al. [21] for a discussion of these liquid column breakup properties.

C. Mean Liquid Surface Streamwise Velocities

To characterize turbulent primary breakup properties along the liquid surface, it is useful to consider the variation of streamwise liquid surface velocities up to the completion of the breakup of the entire column as a whole as a function of distance from the injector exit. This information was obtained by measuring the streamwise velocities of small disturbances on the surface of the liquid jet, using a large number of double-pulse shadowgraphs. The jet exit mean velocity was approximated by the mean bulk velocity, which was calculated from the liquid flow rate. The liquid flow rate was measured by collecting the test liquid injected from the nozzle exit at different injection pressures into a graduated beaker during various time periods. The results from various crossflow conditions are illustrated in Fig. 4. Measured velocities shown in the figure are averaged streamwise liquid surface velocities normalized by the jet exit mean velocity, $\bar{v}_{surf}/\bar{v}_j$. It was found that $\bar{v}_{surf}/\bar{v}_j$ is uniform and independent of the liquid jet condition and the distance from the jet exit up to the fracture point for the present range of q, or

$$\bar{v}_{surf}/\bar{v}_j = 1.0 \qquad (2)$$

Thus, the streamwise liquid surface velocity until the breakup point is essentially equal to the mean streamwise jet velocity at the jet exit, indicating the relatively weak interaction between the streamwise motion of the liquid jet and the gaseous crossflow. Similar behavior was also observed for nonturbulent round liquid jets in gaseous crossflows by Sallam et al. [2].

D. Onset of Turbulent Primary Breakup

Consideration of conditions at the onset of turbulent primary breakup along the liquid surface, allowing for aerodynamic enhancement of the breakup process due to the presence of crossflow, followed the earlier phenomenological analyses of Wu and Faeth [16]. Enhanced aerodynamic primary breakup is associated with effects of pressure drop along the sides of the jet, which is caused by the acceleration of the surrounding gas as it flows around the jet. The analysis involved extending the approach of Wu et al. [15], in which the onset of breakup was determined by conditions in which the momentum of turbulent fluctuations in the liquid was just sufficient to overcome surface tension forces so that ligaments can form, to include aerodynamic contributions of the

crossflow. One such result is reduced pressures along the sides of the liquid jet. The reduced pressure locally decreases the threshold of turbulent fluctuations necessary to overcome the surface tension forces. The effect of the crossflow on the formation of ligaments along turbulent round liquid jets is thus to reduce the minimum ligament diameter when compared with a turbulent jet without crossflow:

$$\frac{1}{2}\rho_L v_{lig}^2 \pi \frac{d_{lig}^2}{4} - \frac{1}{2}C_{sp}\rho_G u_\infty^2 \pi \frac{d_{lig}^2}{4} = C_{si}\sigma\pi d_{lig} \qquad (3)$$

Because d_{lig} must be in the inertial range (see Wu and Faeth [16]), $v_{lig} \sim \bar{v}'(d_{lig}/\Lambda)^{1/3}$, where Λ is the radial (cross-stream) integral length scale and $\Lambda = d/8$ for turbulent pipe flow (Hinze [26]). The location of the onset of breakup follows from the time required for a ligament to grow and produce a drop at its tip due to Rayleigh breakup (see Sec. III.E for more details). The breakup time is converted to a length along the liquid surface based on the assumption that ligaments convect along the liquid surface in the streamwise direction at $\bar{v}_{surf} = \bar{v}_j$, which is justified by the results illustrated in Fig. 4. This phenomenological analysis follows Wu and Faeth [16] and yields the following result for the aerodynamically enhanced streamwise location for the onset of turbulent primary breakup along the liquid surface:

$$(y_i/\Lambda)[1 - C_{sp}(y_i/\Lambda)^{-4/9}We_{L\Lambda}^{2/9}(\rho_G/\rho_L)(u_\infty/\bar{v}_j')^2]^{9/10}$$
$$= C_{yi}We_{L\Lambda}^{-n} \qquad (4)$$

where $n = 4/10$.

This relation, which considers the aerodynamic enhancement of breakup processes, covers both still and crossflowing air regimes (for the Weber numbers studied). For crossflowing conditions, the aerodynamic effects enhance turbulent primary breakup along the sides and the downwind side of the jet, but not on the upwind side, for which liquid turbulence and aerodynamic effects will have competing effects. It follows that the crossflow makes it easier for ligaments to form on the downwind side; that is, the crossflow progressively reduces y_i or progressively increases the ligament diameter corresponding to a particular y_i. The present measurements with and without crossflow are plotted in Fig. 5, according to Eq. (4). Also included are the measurements of Wu et al. [15] for no crossflow. In completing this plot, the values $C_{sp} = -0.07$, $C_{yi} = 1893$, and $n = 0.59$ were obtained to be best-fit values to achieve a correlation between y_i/Λ and the other properties of the breakup process. This selection depends on taking $\bar{v}_j'/\bar{v}_j = 0.03$ for the bulk liquid for fully developed turbulent pipe flow from Hinze [26]. The difference between the theoretical value of $n = 0.40$ and the correlated value of 0.59 is statistically significant, but is not large in view of the approximations used to develop the correlating
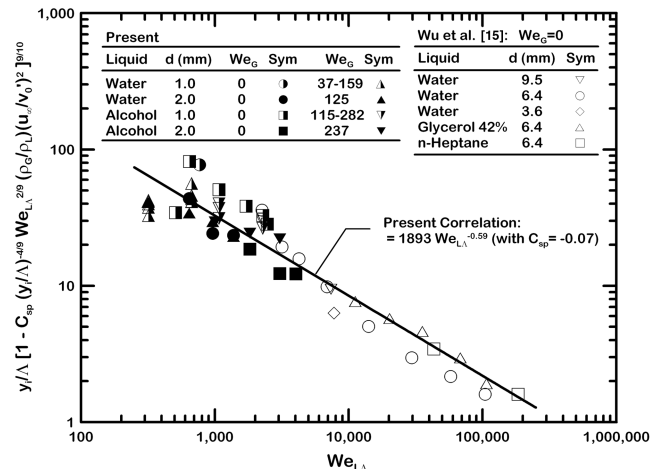

Present						Wu et al. [15]: We$_G$=0		
Liquid	d (mm)	We$_G$	Sym	We$_G$	Sym	Liquid	d (mm)	Sym
Water	1.0	0	◐	37-159	▲	Water	9.5	▽
Water	2.0	0	●	125	▲	Water	6.4	○
Alcohol	1.0	0	◪	115-282	▼	Water	3.6	◇
Alcohol	2.0	0	■	237	▼	Glycerol 42%	6.4	△
						n-Heptane	6.4	□

Present Correlation:
= 1893 We$_{L\Lambda}^{-0.59}$ (with C_{sp} = -0.07)

Fig. 5 Streamwise length to the onset of breakup as a function of the Weber number for turbulent liquid jets in crossflow.

expression (notably, Wu and Faeth [16] found $n = 0.63$ for these measurements, which is very close to the present value). The large value C_{yi} can be anticipated, because [16]

$$C_{yi} = C_{si} 8^{9/10} (\bar{v}_j / \bar{v}'_j)^{9/5} \tag{5}$$

and $\bar{v}_j / \bar{v}'_j$ is a large number for fully developed turbulent pipe flow. For example, taking $\bar{v}'_j / \bar{v}_j = 0.03$ as before yields $C_{si} = 0.5$, which is a number on the order of unity that is expected, based on phenomenological analysis considerations.

E. Ligament and Drop Properties Along the Liquid Surface

An expression for the variation of ligament diameter as a function of distance from the jet exit due to effects of turbulent primary breakup was developed following the approach of Sallam and Faeth [22], in which it was shown that for high-speed jets in still air, the aerodynamic breakup time of ligaments is comparable to the Rayleigh breakup time, indicating that Rayleigh breakup is dominant. Their work employed methods from earlier turbulent primary breakup considerations by Wu et al. [15]. This approach was adopted using the relationship between the diameters of ligaments that are just forming drops at a point (the most prominent ligaments at a point due to their length) and the corresponding diameters of drops formed by Rayleigh breakup of these ligaments. This was done with consideration given to the convection of a ligament along the surface of a turbulent liquid jet for the Rayleigh breakup time required to form a full-length ligament that is ready to produce a drop. Weber [27] showed that the Rayleigh breakup time of a liquid jet having a diameter of d_{lig}, and thus a ligament of similar size under the present assumptions, is as follows:

$$t_r \sim \left(\rho_L d_{\text{lig}}^3 / \sigma\right)^{1/2} + 3\mu_L d_{\text{lig}} / \sigma \tag{6}$$

where the second term on the right-hand side of Eq. (6) accounts for the effects of liquid viscosity to increase the Rayleigh breakup time. For the present conditions, the viscous term in Eq. (6) is small and can be ignored. Then Eq. (6) becomes

$$t_r \sim \left(\rho_L d_{\text{lig}}^3 / \sigma\right)^{1/2} \tag{7}$$

which is independent of the ligament velocity. Then under the assumption that the ligament is simply convected along the liquid surface for the ligament breakup time, the location in which a ligament having a particular diameter reaches its full length is given by

$$y \sim \bar{v}_j t_r \tag{8}$$

Finally, substituting Eq. (7) into Eq. (8) and normalizing the streamwise distance by the radial integral scale Λ yields the following expression for the variation of d_{lig}/Λ with distance from the jet exit:

$$d_{\text{lig}} / \Lambda = C_{\ell y} \left[y / \left(\Lambda W e_{L\Lambda}^{1/2}\right) \right]^{2/3} \tag{9}$$

where $C_{\ell y}$ is a constant of proportionality that should be on the order of unity. Ligaments of interest here are those that form drops at a particular distance from the jet exit; therefore, the ligament diameters increase with increasing distance from the jet exit because larger ligaments require a longer time to develop and break up, as indicated by Eq. (7), and thus require a larger distance from the jet exit, as indicated by Eq. (8).

The present measurements of ligament diameters along the surface of turbulent round liquid jets in crossflowing gases are plotted in Fig. 6, along with the measurements of turbulent round liquid jets in still air by Wu and Faeth [16], following Eq. (9). The best-fit correlation of d_{lig}/Λ according to the variables of Eq. (9), illustrated in Fig. 6, is given by
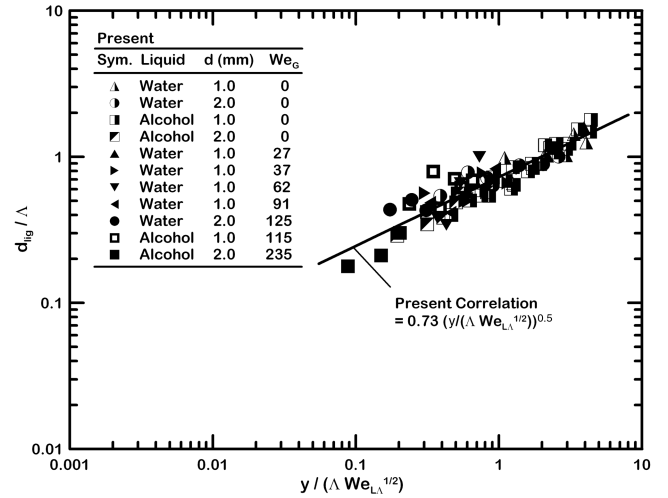

Fig. 6   Ligament diameters of turbulent round liquid jets in crossflow as a function of the normalized streamwise distance.

$$d_{\text{lig}} / \Lambda = 0.73 \left[y / \left(\Lambda W e_{L\Lambda}^{1/2}\right) \right]^{0.5} \tag{10}$$

The difference between the best-fit power of Eq. (10), 0.5, and the theoretical power of Eq. (9), 0.67, is statistically significant but rather modest in view of the approximations of the analysis.

An interesting feature of this result is that ligament properties are clearly dominated by effects of liquid turbulence, with crossflow having no noticeable effect on the correlation at the present test conditions ($We_G < 300$). This is not surprising, however, because Wu and Faeth [16] found negligible aerodynamic effects on turbulent primary breakup when liquid/gas density ratios ρ_L / ρ_G were greater than 500 for relative velocities between the gas and liquid phases, comparable to the present investigation.

Earlier study of turbulent primary breakup of round liquid jets in still gases by Sallam and Faeth [21] suggested that drop formation at the tip of ligaments involves drop diameters comparable to ligament diameters. Then based on the results of Tyler [28], this behavior is characteristic of Rayleigh breakup of ligaments, further justifying the derivation of Eq. (6), and it is reasonable to assume that the SMD of drops formed by ligament breakup are proportional to the corresponding ligament diameter. This implies that

$$\text{SMD} / \Lambda = C_s (d_{\text{lig}} / \Lambda) \tag{11}$$

where C_s should be an empirical constant on the order of unity. Then substituting Eq. (9) into Eq. (11) yields

$$\text{SMD} / \Lambda = C_s C_{\ell y} \left[y / \left(\Lambda W e_{L\Lambda}^{1/2}\right) \right]^{2/3} \tag{12}$$

The present measurements of SMD after turbulent primary breakup along the surface of turbulent round liquid jets in still and crossflowing gases are plotted in Fig. 7, as suggested by Eq. (12), along with earlier measurements of drop sizes after the turbulent primary breakup in still gases by Wu and Faeth [16]. The agreement between the results of Wu and Faeth and the present investigation is excellent and yields the following combined correlation:

$$\text{SMD} / \Lambda = 0.56 \left(y / \left(\Lambda W e_{L\Lambda}^{1/2}\right) \right)^{0.5} \tag{13}$$

Notably, the power in Eq. (13), 0.5, is equal to the power for ligament diameters in Eq. (10) and is not very different from the theoretical power of Eq. (12), 0.67, whereas the coefficient of Eq. (13) is on the order of unity, as expected from phenomenological theory. These results also support the idea that drop formation for turbulent primary breakup at the present conditions occurs by Rayleigh breakup at the tips of ligaments. Moreover, the excellent agreement in Fig. 7 between the present drop sizes of turbulent liquid jet in crossflow and drop sizes of turbulent liquid jet in still air by Wu and Faeth [16]
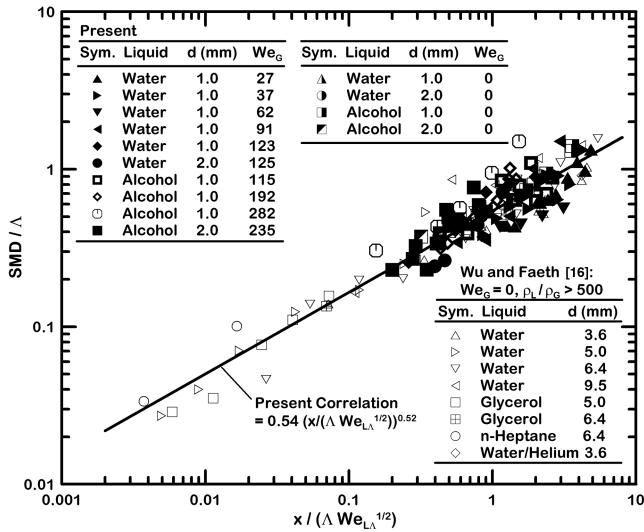
Fig. 7 Drop diameters after primary breakup for turbulent round jets in still and crossflowing gases as a function of the normalized streamwise distance.

supports the present conclusion that the crossflow did not affect the ligament properties that are responsible for creating the droplets along the liquid jet for the present test conditions ($We_G < 300$).

F. Drop Velocities After Turbulent Primary Breakup

Mean streamwise and cross-stream drop velocities after turbulent primary breakup were measured for both still and crossflowing environments. These measurements were obtained close to the tips of ligaments to minimize the effects of drop-velocity relaxation to the ambient velocity. The resulting drop-velocity distributions in the streamwise direction v_p and in the cross-stream direction u_p are illustrated in Fig. 8. Streamwise velocities are plotted for turbulent

Fig. 8 Streamwise and cross-stream drop velocities after breakup as a function of the drop size.

round liquid jets in both still and crossflowing air, whereas cross-stream velocities are plotted only for turbulent round liquid jets in crossflowing air. First of all, it is clear that drop-velocity distributions are uniform and nearly independent of the drop diameter. The velocity correlations of the measurements illustrated in Fig. 8 follow the normalizations by Sallam et al. [2] for drop velocities after primary breakup from nonturbulent round liquid jets in crossflows:

$$\bar{v}_p / \bar{v}_j = 0.75 \tag{14}$$

$$\bar{u}_p / u_L = \bar{u}_p / [(\rho_G / \rho_L)^{1/2} u_\infty] = 4.82 \tag{15}$$

These results indicate drag effects of the gas phase on the drop velocities after breakup that tend to reduce streamwise drop velocities from the streamwise jet velocity and to increase cross-stream drop velocities significantly from the characteristic cross-stream velocity. These results are remarkably similar to findings for primary breakup of nonturbulent round liquid jets in crossflow by Sallam et al. [2]. This suggests that the ambient gas, whether still or crossflow, exerts a significant effect on drop velocities after breakup along both nonturbulent and turbulent liquid surfaces.

G. Liquid Column Breakup as a Whole

The locations of the completion of the breakup of the entire liquid column as a whole in the streamwise and cross-stream directions were measured using pulsed shadowgraph images that were averaged to find mean liquid column breakup lengths with experimental uncertainties (95% confidence) of less than 10%. The analysis followed the approach of Sallam et al. [2]. This was done by associating the time of penetration of elements of the liquid jet with the time of secondary breakup of drops due to shock wave disturbances. Although crossflow-enhanced turbulent primary breakup is the primary mechanism for the drop formation along the liquid jet, the aerodynamic forces cause a deflection of the jet in the crossflow direction and enhance the breakup of the jet as a whole (the location of the fracture point). With the jet element approach, the time required for breakup, t_b, is given by an expression analogous to that used for the secondary drop-breakup times due to shock wave disturbance from Hsiang and Faeth [29]:

$$t_b / t^* = C_{yb} \tag{16}$$

where t^* is the characteristic aerodynamic time of Ranger and Nicholls [30],

$$t^* = (\rho_L / \rho_G)^{1/2} d_j / u_\infty \tag{17}$$

and C_{yb} is an empirical constant associated with the time of breakup of the liquid column having a magnitude on the order of unity. Using an analysis similar to that of Wu et al. [31], the breakup length in the cross-stream direction is given by

$$x_b / d_j = C_{xb} \tag{18}$$

where C_{xb} is an empirical constant associated with the cross-stream penetration of the liquid column having a magnitude on the order of unity.

Measurements of t_b and x_b for turbulent liquid jets are illustrated in Fig. 9, along with results for nonturbulent liquid jets by Sallam et al. [2]. As anticipated from earlier measurements of nonturbulent liquid jets, the ratio t_b / t^* is relatively independent of the Weber number for all test conditions, yielding $C_{yb} = 1.61$ for the present measurements of turbulent liquid jets in crossflows with an experimental uncertainty (95% confidence) of 8% and $C_{yb} = 2.44$ for the measurements of nonturbulent liquid jets in crossflows by Sallam et al. [2]. Measurements of x_b / d_j from the present investigation yield $C_{xb} = 5.20$ for turbulent liquid jets in crossflows, with an experimental uncertainty (95% confidence) of 9%, which is also independent of the Weber number, whereas the measurements of Sallam et al. [2] yielded $C_{xb} = 8.64$ for nonturbulent liquid jets in
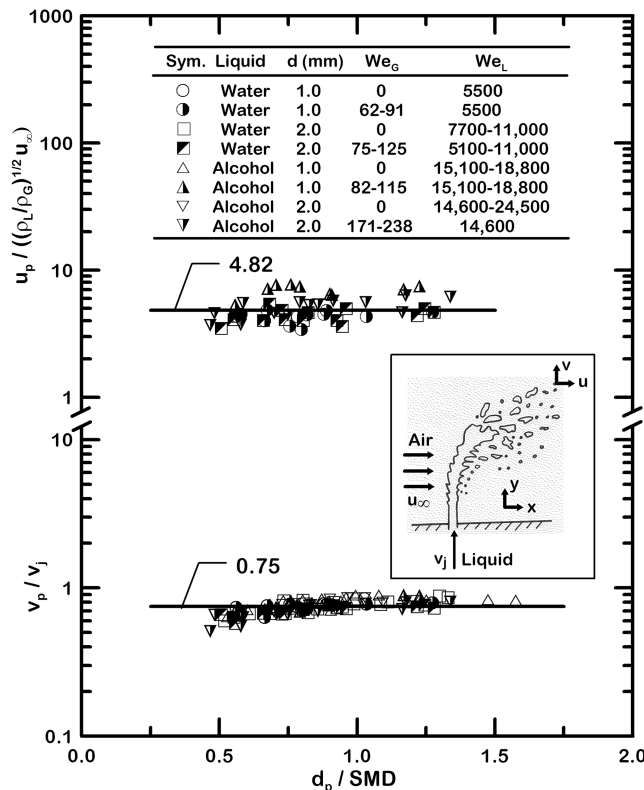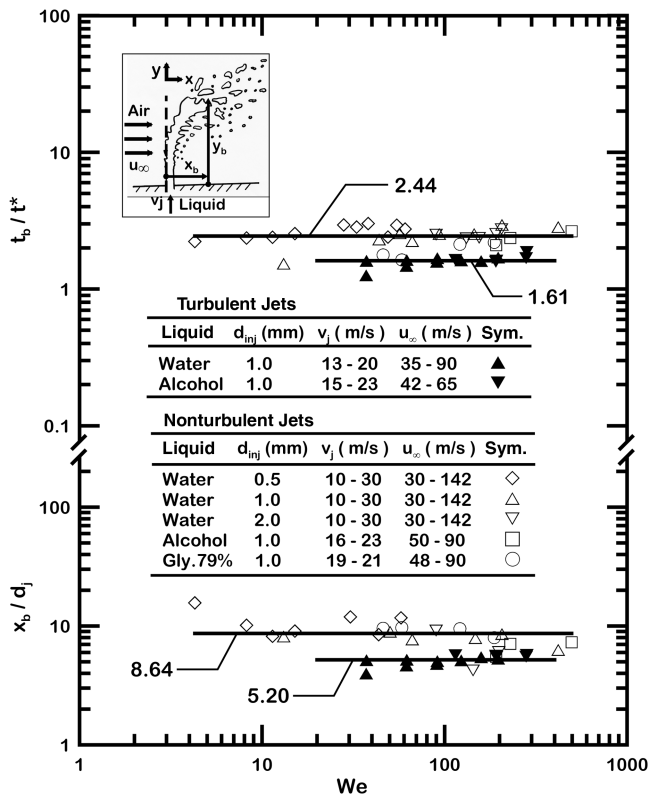
Fig. 9 Location of end of liquid jets in the streamwise and cross-stream directions during primary breakup of turbulent and nonturbulent round liquid jets in gaseous crossflow.

Fig. 10 Mean surface efficiency factors as functions of normalized streamwise distance for turbulent round jets in crossflow.

crossflows. It is noteworthy that the values of both C_{yb} and C_{xb} for turbulent liquid jets in crossflows are smaller than those for nonturbulent liquid jets in crossflows from Sallam et al. [2]. The presence of turbulence in the liquid jets thus enhances the process of liquid column breakup as a whole, resulting in shorter breakup times and lengths of turbulent liquid jets in crossflows, compared with nonturbulent liquid jets in crossflows.

H. Liquid Breakup Rates Due to Turbulent Primary Breakup

The flux of liquid drops relative to the liquid surface due to turbulent primary breakup along the liquid surface was also studied during the present investigation for the shear breakup regime. The evidence of relatively strong effects of crossflow on drop velocities after turbulent primary breakup suggested that this would best be done using the approach of Sallam et al. [2] for nonturbulent primary breakup in crossflow. With this approach, drops formed by primary breakup are assumed to leave the liquid column over its downstream half as opposed to the entire periphery, which was the approach used for breakup of turbulent liquid jets in still gases [21]. Thus, averaging the liquid removal rate over this downstream projected area to find the average mass flux of liquid drops leaving the liquid column, $\dot{m}_L''$, the liquid surface breakup efficiency factor ε is defined as follows:

$$\varepsilon = \dot{m}_L'' / (\rho_L \bar{u}_p) \tag{19}$$

where the limit $\varepsilon = 1$ represents conditions in which liquid drops form in a continuous manner over all of the downstream projected area of the liquid.

The mass flux $\dot{m}_L''$ was determined by measuring the volume (and hence the mass) of the droplets leaving the liquid column per unit jet-projected-area per unit time using the double-pulsed holograms. The present measurements of ε for primary breakup of turbulent round liquid jets in crossflowing air are plotted as a function of dimensionless streamwise length $y_{b,\text{laminar}}$ in Fig. 10, along with earlier results for nonturbulent round liquid jets in crossflowing air by Sallam et al. [2]. It should be noted that according to Fig. 9, liquid
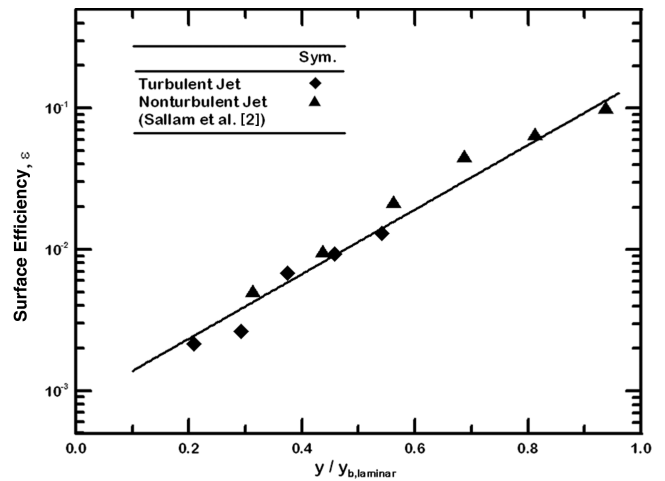
column breakup lengths of turbulent round liquid jets are actually shorter than those of nonturbulent round liquid jets at corresponding Weber number conditions with a ratio of nonturbulent/turbulent breakup length $y_{b,\text{laminar}}/y_b = 1.5$. The streamwise length on the x axis of Fig. 10 was normalized by the liquid column breakup length of nonturbulent round liquid jets with corresponding Weber number $y_{b,\text{laminar}} = 1.5 y_b$ to allow comparison of the present measurements of surface efficiency for turbulent round liquid jets in crossflows with measurements of Sallam et al. [2] for nonturbulent round liquid jets in crossflows. The present measurements for turbulent round liquid jets agree very well with earlier results for nonturbulent round liquid jets, and the best-fit correlation of ε for the present measurements of turbulent round liquid jets and earlier measurements of nonturbulent round liquid jets by Sallam et al. [2] is as follows:

$$\varepsilon = 7.76 \times 10^{-4} \exp(5.5 y / y_{b,\text{laminar}}) \tag{20}$$

The present measurements of ε started at a smaller dimensionless streamwise length, because the onsets of breakup for turbulent round liquid jets happen closer to the jet exit due to the effect of turbulence. The present measurements of ε also ended at a smaller dimensionless streamwise length because the liquid column breakup lengths as a whole for turbulent round liquid jets are shorter than for nonturbulent round liquid jets. Values of ε are small at the onsets of breakup but increase toward unity as the end of the liquid column is approached, similar to the results for nonturbulent round liquid jets [2].

I. Liquid Column Trajectories

The liquid jet trajectory was considered next because drops formed at the surface of the liquid jet naturally emanate from locations along the jet in the x–y plane. In this case, simplified analysis following Wu et al. [31] and Sallam et al. [2] was used, considering flow in the shear breakup regime. The analysis was based on convection at the jet exit velocity in the jet streamwise direction. The results for cross-stream direction were based on conservation of momentum, assuming a constant drag coefficient based on the jet exit diameter for the shear breakup regime. Under these assumptions, the expression for the trajectory is as follows [31]:

$$y/(d_j q) = \sqrt{\pi/C_D} [x/(d_j q)]^{1/2} \tag{21}$$

Sallam et al. [2] grouped the measurements and predictions according to the breakup regimes and determined respective drag coefficients C_D for each breakup regime (with $C_D = 3$ for shear breakup). The present measurements of liquid column trajectories of turbulent round liquid jets in crossflows in the shear breakup regime are illustrated in Fig. 11. Measurements agree very well with the theoretical prediction and earlier results for nonturbulent round liquid jets in the shear breakup regime by Sallam et al., yielding
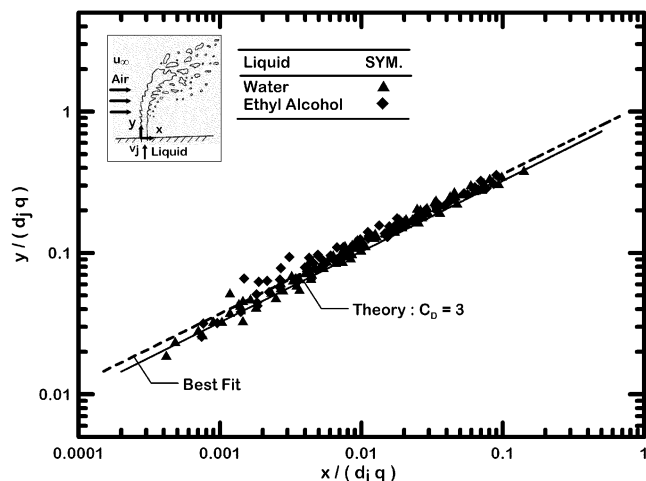
Fig. 11 Liquid column trajectories in the streamwise and cross-stream directions during primary breakup of turbulent round liquid jets in gaseous crossflow.

$C_D = 3$ as well. The presence of turbulence in liquid jets has little effect on liquid column trajectories, whereas the aerodynamic effects of crossflow are dominant in determining liquid column trajectories.

IV.   Conclusions

This investigation considered the formation of ligaments and drops along the surface of turbulent round liquid jets in uniform air crossflows at normal temperature and pressure. Test conditions included water and ethyl alcohol jets with fully developed turbulent pipe flow properties injected normal to the crossflow for the following ranges of test variables: crossflow Weber numbers based on gas properties of 0–282, streamwise Weber numbers based on liquid properties of 1400–32,200, liquid/gas density ratios of 683 and 845, liquid jet exit Reynolds numbers of 7100–48,200, and Ohnesorge numbers less than 0.12. The major conclusions of the study are as follows:

1) The onset of turbulent primary breakup always occurred at some distance from the jet exit but approached the jet exit at large $We_{L\Lambda}$. The formation of ligaments and drops was enhanced by the presence of crossflow, which reduces the pressure along the sides of the liquid jet and thereby accelerates the onset of breakup.

2) Ligament and drop SMDs increased with increasing distance from the jet exit and became comparable to the radial integral scale of the liquid turbulence as the end of the liquid column was approached.

3) The correlation between drop SMD and streamwise distance along the liquid jet was not affected by the crossflow, suggesting that the turbulence in the liquid jet yields the primary breakup mechanism even in the presence of crossflow for the present test conditions.

4) Drop velocities after turbulent primary breakup in crossflow were independent of drop size and similar to drop velocities after nonturbulent primary breakup in crossflow. Streamwise drop velocities were comparable to mean streamwise liquid jet velocities and cross-stream drop velocities were somewhat larger than the characteristic cross-stream velocity.

5) The mean drop mass flux over the downstream projected area of the liquid column due to turbulent primary breakup at the liquid surface was in good agreement with earlier measurements of nonturbulent round liquid jets in crossflows by Sallam et al. [2] when normalized by the liquid column breakup length of nonturbulent jets with corresponding Weber number.

6) Breakup times and distances of the turbulent liquid column as a whole were smaller than the results for nonturbulent liquid jets by Sallam et al. [2], indicating enhancing effects of liquid turbulence on liquid column breakup.

The features observed here are attributed to the interaction of the turbulent eddies within the liquid jet with the jet's free surface. At high liquid jet Reynolds numbers, these turbulent eddies would have enough kinetic energy to cause surface breakup not only at the downwind side, but also at the upwind side, despite the presence of the gaseous crossflow. An increase in the crossflow velocity, however, equivalent to a decrease in the liquid/gas momentum ratio, could possibly suppress the upwind surface breakup when the energy of turbulent eddies in the liquid jet is not large enough to overcome the combination of liquid surface tension forces and the pressure forces exerted by the gaseous crossflow. This mechanism merits further investigation.

References

[1] Mazallon, J., Dai, Z., and Faeth, G. M., "Primary Breakup of Nonturbulent Round Liquid Jets in Gas Crossflows," *Atomization and Sprays*, Vol. 9, No. 3, 1999, pp. 291–311.

[2] Sallam, K. A., Aalburg, C., and Faeth, G. M., "Breakup of Round Nonturbulent Liquid Jets in Gaseous Crossflow," *AIAA Journal*, Vol. 42, No. 12, 2004, pp. 2529–2540.

[3] Aalburg, C., van Leer, B., Faeth, G. M., and Sallam, K. A., "Properties of Nonturbulent Round Liquid Jets in Uniform Gaseous Crossflows," *Atomization and Sprays*, Vol. 15, No. 3, 2005, pp. 249–270.

[4] Fuller, R. P., Wu, P.-K., Kirkendall, K. A., and Nejad, A. S., "Effects of Injection Angle on Atomization of Liquid Jets in Transverse Airflow," *AIAA Journal*, Vol. 38, No. 1, 2000, pp. 64–72.

[5] De Juhasz, K. J., Zahn, O. F., Jr., and Schweitzer, P. H., "On the Formation and Dispersion of Oil Sprays," *Bulletin No. 40, Engineering Experimental Station*, Pennsylvania State University, University Park, PA, 1932.

[6] Lee, D. W., and Spencer, R. C., "Preliminary Photomicrographic Studies of Fuel Sprays," NACA, Rept. 424, Washington, D.C., 1933.

[7] Lee, D. W., and Spencer, R. C., "Photomicrographic Studies of Fuel Sprays," NACA Rept. 454, Washington, D.C., 1933.

[8] Schweitzer, P. H., "Mechanism of Disintegration of Liquid Jets," *Journal of Applied Physics*, Vol. 8, 1937, pp. 513–521.

[9] Chen, T.-F., and Davis, J. R., "Disintegration of a Turbulent Water Jet," *Journal of the Hydraulics Division, American Society of Civil Engineers*, Vol. 90, No. 1, 1964, pp. 175–206.

[10] Grant, R. P., and Middleman, S., "Newtonian Jet Stability," *AIChE Journal*, Vol. 12, No. 4, July 1966, pp. 669–678.

[11] Phinney, R. E., "The Breakup of a Turbulent Jet in a Gaseous Atmosphere," *Journal of Fluid Mechanics*, Vol. 60, No. 4, Oct. 1973, pp. 689–701.

[12] McCarthy, M. J., and Malloy, N. A., "Review of Stability of Liquid Jets and the Influence of Nozzle Design," *Chemical Engineering Journal*, Vol. 7, No. 1, 1974, pp. 1–20.

[13] Hoyt, J. W., and Taylor, J. J., "Waves on Water Jets," *Journal of Fluid Mechanics*, Vol. 83, No. 1, Nov. 1977, pp. 119–123.

[14] Hoyt, J. W., and Taylor, J. J., "Turbulence Structure in a Water Jet Discharging in Air," *Physics of Fluids*, Vol. 20, No. 10, 1977, pp. S253–S257.

[15] Wu, P.-K., Tseng, L.-K., and Faeth, G. M., "Primary Breakup in Gas/Liquid Mixing Layers for Turbulent Liquids," *Atomization and Sprays*, Vol. 2, No. 3, 1992, pp. 295–317.

[16] Wu, P.-K., and Faeth, G. M., "Aerodynamic Effects on Primary Breakup of Turbulent Liquids," *Atomization and Sprays*, Vol. 3, No. 3, 1993, pp. 265–289.

[17] Wu, P.-K., Miranda, R. F., and Faeth, G. M., "Effects of Initial Flow Conditions on Primary Breakup of Nonturbulent and Turbulent Round Liquid Jets," *Atomization and Sprays*, Vol. 5, No. 2, 1995, pp. 175–196.

[18] Wu, P.-K., and Faeth, G. M., "Onset and End of Drop Formation Along the Surface of Turbulent Liquid Jets in Still Gases," *Physics of Fluids A*, Vol. 7, No. 11, 1995, pp. 2915–2917.

[19] Dai, Z., Chou, W.-H., and Faeth, G. M., "Drop Formation Due to Turbulent Primary Breakup at the Free Surface of Plane Liquid Wall Jets," *Physics of Fluids*, Vol. 10, No. 5, 1998, pp. 1147–1157.

[20] Sallam, K. A., Dai, Z., and Faeth, G. M., "Drop Formation at the Surface of Plane Turbulent Liquid Jets in Still Gases," *International Journal of Multiphase Flow*, Vol. 25, Nos. 6–7, Sept. 1999, pp. 1161–1180.

[21] Sallam, K. A., Dai, Z., and Faeth, G. M., "Liquid Breakup at the Surface of Turbulent Round Liquid Jets in Still Gases," *International Journal of Multiphase Flow*, Vol. 28, No. 3, 2002, pp. 427–449.

[22] Sallam, K. A., and Faeth, G. M., "Surface Properties During Primary Breakup of Turbulent Liquid Jets in Still Air," *AIAA Journal*, Vol. 41, No. 8, 2003, pp. 1514–1524.

[23] Simmons, H. C., "The Correlation of Drop-Size Distributions in Fuel Nozzle Sprays," *Journal of Engineering for Power*, Vol. 99, No. 3, 1977, pp. 309–319.

[24] Schlichting, H., *Boundary Layer Theory*, 4th ed., McGraw–Hill, New York, 1960, pp. 72–73 and 599.

[25] Lange, N. A., *Handbook of Chemistry*, 8th ed., Handbook Publishers, Inc., Sandusky, OH, 1984, pp. 13–17.

[26] Hinze, J. O., *Turbulence*, 2nd ed., McGraw–Hill, New York, 1975, pp. 724–742.

[27] Weber, C., "Zum Zerfall eines Flussigkeitsstrahles," *Zeitschrift Angewesen Mathematik and Mechanik*, Vol. 2, 1931, pp. 136–141.

[28] Tyler, E., "Instability of Liquid Jets," *Philosophical Magazine*, Vol. 16, 1933, pp. 504–518.

[29] Hsiang, L.-P., and Faeth, G. M., "Drop Deformation and Breakup Due to Shock Wave and Steady Disturbances," *International Journal of Multiphase Flow*, Vol. 21, No. 4, 1995, pp. 545–560.

[30] Ranger, A. A., and Nicholls, J. A., "The Aerodynamic Shattering of Liquid Drops," *AIAA Journal*, Vol. 7, No. 2, 1969, pp. 285–290.

[31] Wu, P.-K., Kirkendall, K. A., Fuller, R. F., and Nejad, A. S., "Breakup Processes of Liquid Jets in Subsonic Crossflows," *Journal of Propulsion and Power*, Vol. 13, No. 1, 1997, pp. 64–73.

S. Aggarwal
Associate Editor